Carbon Dioxide Interactions with Crystalline and Amorphous Ice Surfaces

Patrik U. Andersson,[†] Mats B. Någård,[†,‡] Georg Witt,[§] and Jan B. C. Pettersson*[,†]

Atmospheric Science, Department of Chemistry, Göteborg University, SE-412 96 Göteborg, Sweden, and Department of Meteorology, Stockholm University, SE-106 91 Stockholm, Sweden

Received: February 13, 2004; In Final Form: March 12, 2004

Carbon dioxide interactions with crystalline and amorphous water ice have been studied by time-resolved molecular beam techniques. CO_2 collisions at thermal kinetic energies with ice in the temperature range 100−160 K result in efficient trapping on the ice surface followed by desorption. The desorption kinetics on crystalline ice at 100−125 K are well described by the Arrhenius equation with an activation energy of 0.22 ± 0.02 eV and a preexponential factor of $10^{13.32\pm0.57}$ s^{-1}. Below 120 K, CO_2 populates strongly bonded sites on amorphous ice, resulting in surface residence times on the order of minutes at 100 K, and the desorption data can in this case not be explained by a simple first-order process. The results are compared to previous studies of gas−ice interactions, and the implications for heterogeneous processes in the terrestrial atmosphere are discussed.

Introduction

Molecular interactions with water ice are of fundamental importance in several disciplines, including atmospheric science and interstellar chemistry, and the dynamics of gas−ice interactions have recently received considerable attention. The collision and accommodation of molecules on an ice surface is the first step in any heterogeneous process. During a collision a molecule may be trapped on the surface or directly scatter back into the gas phase. The trapped molecules may thermally desorb from the surface, diffuse in the surface layer or into the bulk, or continue to react. We have previously employed molecular beam techniques to investigate Ar collisions with water ice.[1] The results showed that the collisions are highly inelastic and characterized by efficient transfer of energy to surface modes, which leads to a large energy loss for directly scattered molecules. Under thermal conditions Ar atoms are efficiently trapped, but rapidly leave the surface by desorption because of the low energy of binding to the surface. Gotthold and Sitz[2] studied the scattering of N_2 from ice with state-resolved detection of the flux from the surface. For beam incidence in the surface normal direction, scattering was found to be entirely dominated by trapping−desorption for kinetic energies below 0.3 eV, while an inelastic scattering channel opened up at higher incident energies. Studies of the reactive HCl−ice system[3] showed that the surface collisions are highly inelastic with large energy loss observed for the directly scattered flux, similar to the results for the Ar−ice and N_2−ice systems. The data for the energy loss as a function of scattering angle showed that energy transfer is substantial both parallel and perpendicular to the surface plane during surface collisions. Contrary to the argon−ice system, trapped HCl molecules form strong bonds with the ice surface, and the dominating outcome of the surface interaction is a loss of HCl by sticking to the surface. Similar results were obtained by Rieley et al.[4] and Isakson and Sitz[5] for HCl and HBr on ice.

Molecular dynamics (MD) simulations have been carried out for some of the systems studied by molecular beam techniques. Bolton et al.[6] performed classical MD simulations on Ar scattering from ice and found that the initial kinetic energy is effectively taken up by the ice surface, and rapidly removed from the impact site. Bolton and Pettersson[7] have also characterized the trapping−desorption and thermal surface penetration by diffusion and found that up to 36% of the argon atoms penetrate the ice surface and diffuse into subsurface interstitial sites as a result of thermally produced disorder in the topmost bilayer of the ice. Classical MD simulations of HCl on ice by Clary and Kroes[8] gave unity sticking coefficients under thermal conditions, and this was also the result from a mixed quantum-classical treatment of HCl on ice by Wang and Clary.[9] In an MD study, Al-Halabi et al.[10] also showed that HCl may penetrate the ice surface by a direct mechanism at high incident energies.

In the present study, CO_2 interactions with water ice surfaces are studied using molecular beam techniques. The experimental method allows for detailed investigations of interaction between molecules and ice surfaces under single-collision conditions. Carbon dioxide has a mass similar to those of Ar and HCl, but the binding energy for the CO_2−ice system is expected to be intermediate between those of the weakly bound Ar−ice and strongly bound HCl−ice systems. We characterize trapping probability and desorption kinetics in the surface temperature range 100−160 K. The results are compared to those of previous studies of gas−ice interactions, and the implications for heterogeneous processes in the atmosphere are discussed. Bryson and Levenson[11] have previously studied CO_2 interactions with amorphous ice at 72−78 K, and they concluded that CO_2 was reflected from the surface if the temperature was larger than 74 K. They also estimated an activation energy for desorption of 0.26 eV from temperature-programmed desorption of a CO_2 layer from ice in the temperature range 75−90 K. In related work the sublimation of CO_2/H_2O ices was also followed by mass spectrometry and IR spectroscopy.[12−14]

* To whom correspondence should be addressed. Phone: +46 31 772 28 28. Fax: +46 31 772 31 07. E-mail: janp@phc.chalmers.se.
[†] Göteborg University.
[‡] Present address: Physical and Computational Chemistry, DMPK and Bioanalytical Chemistry, AstraZeneca R&D Mölndal, SE-431 83 Mölndal, Sweden.
[§] Stockholm University.

10.1021/jp049346c CCC: $27.50
Published on Web 05/04/2004

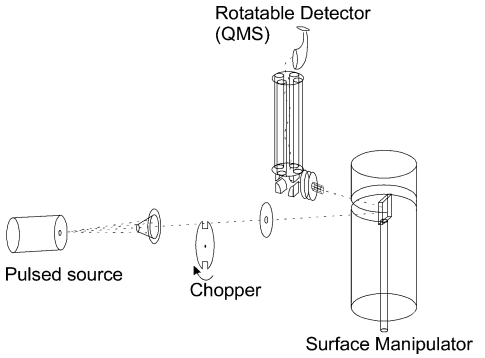

Figure 1. A schematic representation of the molecular beam−surface scattering apparatus used to study CO_2 collisions with water ice surfaces.

Experimental Section

The molecular beam−surface scattering apparatus used to study CO_2 interactions with ice surfaces has been described in detail elsewhere,[1,3] and is only briefly presented here. The apparatus is schematically shown in Figure 1. A pulsed molecular beam source in the first chamber generated pulses with a repetition frequency of 20−61 s^{-1} in the present experiments. Beams were produced using pure CO_2 (purity 99.998%) at a source pressure of typically 1.2 bar, which gave an average kinetic energy of 0.10 eV and a dimer concentration of less than 0.5% in the beam. The pulses were synchronized with a chopper in the second chamber to select the central part of each pulse, giving square-wave-like beam pulses with a width of 90−540 μs depending on the chopper speed being used.

The molecular beam collided with an ice surface in the center of the main scattering chamber. A 12 × 12 mm graphite surface was used as a substrate for ice buildup. The sample can be cooled by liquid nitrogen and heated by irradiation, giving a surface temperature range of 100−750 K with fluctuations of less than 0.2 K. The sample is surrounded by a cylindrical chamber with a diameter of 90 mm, and a slit opening in the cylinder allows the molecular beam to reach the surface and the flux from the surface to reenter into the main chamber. By introducing the cylinder, a low pressure can be maintained in the main chamber (5×10^{-9} mbar) while the ice surface is surrounded by a partial water vapor pressure of up to 10^{-4} mbar. The arrangement makes it possible to maintain an ice surface in dynamic equilibrium at temperatures where the ice undergoes rapid evaporation and condensation.

The flux from the ice surface is detected by a differentially pumped quadrupole mass spectrometer (QMS) that is rotatable around the ice surface. The setup allows for angular resolved time-of-flight measurements with a resolution of $\leq \pm 1°$ in the plane defined by the beam and the surface normal. CO_2^+ ions generated by electron bombardment in the QMS were mass selected and thereafter detected by pulse-counting and stored on a multichannel scaler with a dwell time of 10 μs.

Ice surfaces were built on the graphite substrate by deposition of water vapor, which was introduced into the cylindrical chamber through a leak valve. The water was of Millipore quality (>10 MΩ m), further purified by several freeze−pump−thaw cycles, and stored in a stainless steel container. The initial buildup of ice was performed at a surface temperature of 155 K, and the water vapor pressure around the surface was adjusted to give a buildup rate of 3 monolayers/s (MLs/s). This produces stable crystalline ice I. Ice I exists as cubic and hexagonal ice,[15,16] the hexagonal phase of which is the most stable form at all temperatures, but the formation of cubic ice is kinetically favored under the conditions employed in the present study.[15,16] The structure of the uppermost surface layer is very similar for the two phases. The ice thickness was measured by detecting the reflectance of a diode laser beam directed at the ice surface.[17] The sinusoidal intensity profile produced by interference of the scattered light during ice buildup was recorded by a diode and used to deduce the ice thickness. About 1500 ML of ice were initially built up before the CO_2 beam was turned on. During CO_2 exposure, the water vapor around the surface was either maintained or turned off, which enabled us to perform scattering experiments with both amorphous and crystalline ice. The amorphous ice surface was grown on the initially formed crystalline ice by water deposition at temperatures lower than 130 K. The CO_2 beam flux at the surface was estimated to be about 0.02 ML/s. This estimate was obtained by first recording the pressure increase in the scattering chamber using nitrogen gas in the beam and by using an estimate of the effective pumping speed. The mass spectrometer flux of CO_2 was thereafter compared with the mass spectrometer flux of nitrogen taking into account the difference in ionization probability for the two gases.

Results

We have studied CO_2 collisions with crystalline and amorphous ice at surface temperatures $T_s = 100-160$ K. The experimental results consist of time-of-flight spectra for the CO_2 flux from the ice surface, and all results presented here were obtained using an incident angle $\theta_i = 45°$ with respect to the surface normal and an incident average kinetic energy $E = 0.10$ eV.

Figure 2 shows time-of-flight spectra for CO_2 scattering from crystalline and amorphous ice at different surface temperatures. The spectra were measured in the surface normal direction. The data for crystalline ice were taken with the water inlet turned off. As concluded in previous studies,[1,3] the ice surface remains stable for several hours under these conditions, and the ice only evaporates slowly at the highest temperatures employed. This is further confirmed by the fact that no long-term effects were observed during several hours of CO_2−ice experiments. The spectra show broad peaks that become broader with decreasing temperature. The distributions observed for surface temperatures higher than 125 K are the results expected for thermal desorption, with essentially zero surface residence time, from an ice surface at a given surface temperature. The same distribution was observed also for other scattering angles than the surface normal direction, indicating that no direct scattering of CO_2 occurs under these conditions. We conclude that under the conditions used in this work the surface interaction is completely dominated by trapping of CO_2 to the crystalline ice surface followed by rapid desorption. The distributions in Figure 2 become significantly broader for $T_s \leq 125$ K, indicating that the data are influenced by a finite residence time for CO_2 on the surface. Experiments with amorphous ice surfaces were carried out with a constant surface buildup rate of 3 ML/s. This produces crystalline ice at temperatures above 130 K, and the time-of-flight spectra are identical to the data for crystalline ice at 130−160 K. However, there is a clear difference between the two types of data at surface temperatures lower than 130 K. The total CO_2 flux from the amorphous ice surface is considerably lower than for crystalline ice, and the residence time on the surface is longer.

The time-of-flight data have been simulated assuming that CO_2 thermally desorbs from the ice surface at a rate described by first-order desorption. The velocity distribution of the

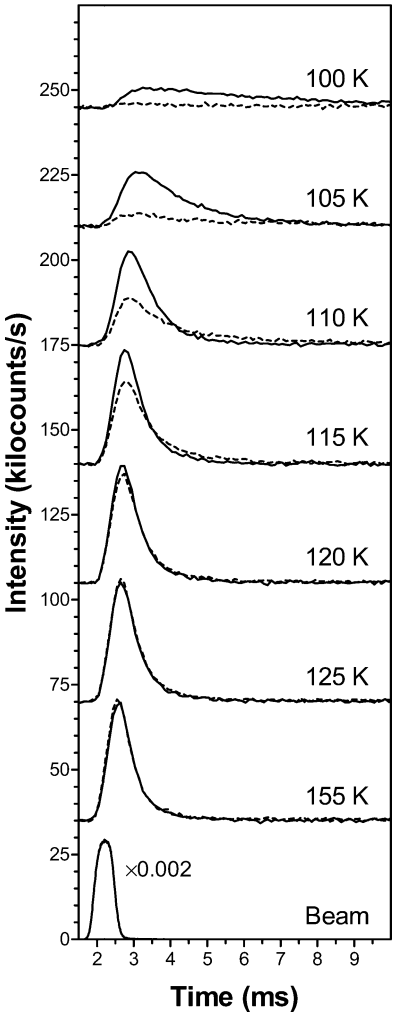

Figure 2. Time-of-flight spectra for CO_2 emitted from ice surfaces at 100−155 K at two different ice buildup rates, 0 ML/s (—) and 3 ML/s (---). The emitted flux was measured in the surface normal direction. The beam measurement was obtained by moving the surface out of the beam and positioning the detector in the beam line, and the obtained distribution is equivalent to elastic scattering from the surface. The incident kinetic energy was 0.10 eV, and the incident angle was 45°.

desorbing flux is described by

$$F_{TD}(v) = c_1 v^2 \exp(-mv^2/2k_B T_s) \quad (1)$$

where v is the velocity, c_1 is a scaling factor, m is the CO_2 mass, and T_s is the surface temperature. The distribution takes into account that the mass spectrometer is density sensitive. The residence time distribution for CO_2 on the surface is described by

$$F_{RES}(t) = \exp(-kt) \quad (2)$$

where t is the residence time and k is the first-order desorption rate constant. Equation 1 is converted into a time-of-arrival distribution and is thereafter fitted to the experimental results by varying c_1, while T_s is kept constant at the surface temperature, and convoluting over the CO_2 density on the ice surface, which is described by the beam profile at the surface and the rate constant k. Examples of fits to the experimental data are shown in Figure 3 for three different temperatures. Using crystalline ice, the fitted curves are in excellent agreement with the experimental results for all temperatures. For amorphous ice surfaces the fitted curves agree well with the experimental results at temperatures above 120 K. At lower temperatures the data for amorphous ice are not as well described by the simulations, indicating that a simple first-order process is not sufficient to explain the results. Figure 4 shows an Arrhenius plot of the desorption rate coefficients obtained from fits to the experimental data. The data for crystalline ice are well described by a straight line giving an activation energy of 0.22 ± 0.02 eV and a preexponential factor of $10^{13.32\pm0.57}$ s^{-1} (least-squares fitting, 95% confidence interval). The average lifetimes on the surface range from 25 μs at 125 K to 3.3 ms at 100 K.

Figure 5 shows the fraction of the incoming CO_2 flux that is emitted from the ice within the total measurement time of 15 ms. The data are obtained by integration of the total desorbing flux observed in time-of flight spectra, taking into account that the detection probability is inversely proportional to the velocity. The absolute scale was fixed by a separate experiment where the desorbing flux of CO_2 from a clean graphite surface was determined. The reflectivity is close to unity at temperatures above 115 K for both amorphous and crystalline ice; i.e., all incoming CO_2 molecules desorb within 15 ms. At lower temperatures the reflectivity remains high for crystalline ice down to 105 K, and drops to 0.6 at 100 K. This decrease is mainly due to the fact that desorption is not completed within the total time limit of 15 ms. For amorphous ice, the drop in desorbing flux with decreasing temperature is substantial and the reflectivity reaches about 0.1 at 100 K. In addition, the reflectivity from amorphous ice is found to stay low when the vapor deposition of water is turned off, indicating that the ice buildup rate is of negligible importance. We conclude that a considerable fraction of the CO_2 is trapped in or on the amorphous ice structure, while this is not an important process on the crystalline surface.

Additional temperature-programmed desorption (TPD) experiments were performed to determine the fate of CO_2 trapped in the amorphous ice at 100 K. A temperature ramp of 10 K/min was started 1 min after the CO_2 dosing was turned off, and mass peaks at m/z = 17, 44, 62, and 63, corresponding to OH^+, CO_2^+, HCO_3^+, and $H_2CO_3^+$, were followed. No signal was found at m/z = 62 and 63, indicating that H_2CO_3 does not desorb from the ice surface. A CO_2 peak was observed in connection with the evaporation of H_2O at temperatures above 170 K. When the temperature ramp was instead started 5 min after CO_2 dosing was turned off, no CO_2 was observed. This indicates that the residence time for CO_2 trapped in the amorphous ice is on the order of a few minutes. Assuming Arrhenius behavior and a frequency factor of 10^{13} s^{-1} for desorption, this residence time corresponds to a desorption activation energy of about 0.3 eV. In a separate TPD experiment with crystalline ice, no CO_2 evaporation was observed in the temperature range 100−200 K.

Discussion

The effective trapping of CO_2 on the ice surface is in agreement with previous results for Ar,[1] N_2,[2] and HCl[3] interacting with ice under similar conditions, and the study confirms the fact that molecules in general will be efficiently accommodated on ice surfaces under thermal conditions. The activation energy of 0.22 ± 0.02 eV and a preexponential factor of $10^{13.32\pm0.57}$ s^{-1} determined for CO_2 desorption from crystalline ice at 100−125 K are comparable with earlier data. Bryson and Levenson[11] used temperature-programmed desorption of a CO_2 layer from ice to estimate an activation energy for desorption

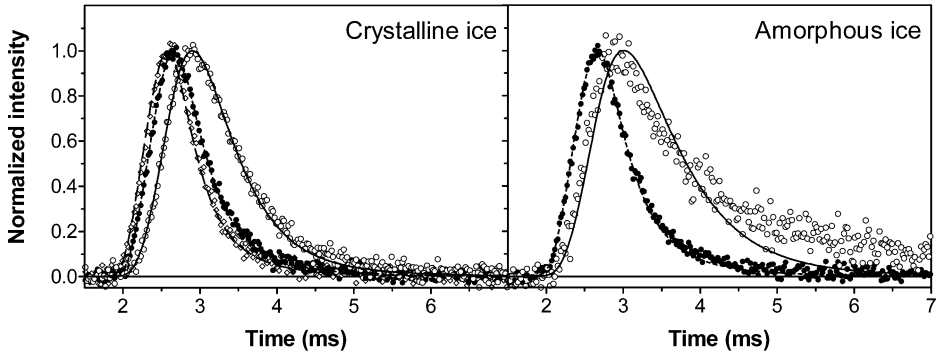

Figure 3. Experimental time-of-flight distributions for CO_2 emitted from crystalline and amorphous ice at 110 K (○), 125 K (●), and 155 K (◇), and fits to the data following the procedure described in the text. For 155 K, the surface residence time was set to zero in the fit. At 125 K a surface residence time of 29 μs was obtained for both crystalline and amorphous ice, and at 110 K residence times of 290 and 500 μs were obtained for crystalline and amorphous ice, respectively.

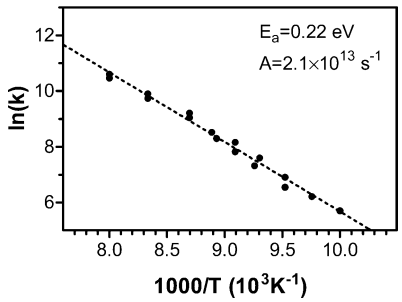

Figure 4. Arrhenius plot of rate coefficients for desorption of CO_2 from crystalline ice.

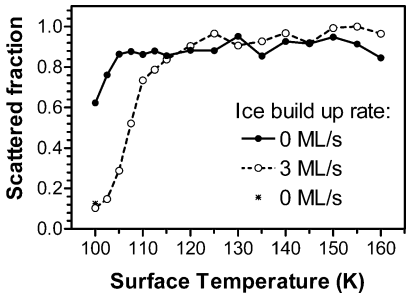

Figure 5. Fraction of the incoming CO_2 flux that is emitted from the ice within a total measurement time of 15 ms. Two different buildup rates were used: 0 ML/s (●) and 3 ML/s (○). The result obtained for amorphous ice after the water was turned off at 100 K is also included (∗). The incident kinetic energy was 0.10 eV, and the incident angle was 45°.

of 0.26 eV in the temperature range 75−90 K. The determination was based on the assumptions that the activation energy was independent of surface coverage and that the preexponential factor was 10^{13} s^{-1}. The second assumption is verified by the data from the present study.

Kay and co-workers have studied the uptake of several gases (N_2, O_2, CO, CH_4, Ar) on and in amorphous ice in the temperature range 22−140 K.[18−21] They found that the underlying substrate, the direction of the incident H_2O molecules during ice buildup, and the surface temperature influence the properties of the amorphous ice structure, and therefore also the gas uptake capability. Under the conditions used in this paper, i.e., background H_2O dosing and growth on an initially crystalline structure at temperatures above 100 K, they obtained uptakes of approximately 1 ML. When lower ice buildup temperatures were used, the uptake increased linearly with ice thickness. By comparing the H_2O and CO_2 intensities in our TPD experiments, we find that about 10 MLs of CO_2 are released upon heating. The difference in gas uptake between the present study and the work by Kay and co-workers may be explained by the higher ice buildup rate used here (1 order of magnitude higher), which could have an effect on the amorphous ice properties. Another potentially important factor is the relatively strong interaction energy for the CO_2−ice system compared to the systems investigated by Kay and co-workers, which should favor gas uptake in the amorphous structure.

The sublimation of CO_2/H_2O ices has previously been studied by mass spectrometry and IR spectroscopy.[12−14] CO_2 release from the ice formed at 25−30 K was observed to be strongly dependent on the initial $[CO_2]/[H_2O]$ ratio.[14] During TPD at 3 K/min, a ratio of 3 gave CO_2 sublimation beginning at about 80 K and peaking at 98 K, with a second larger release peaking at 112 K. As the initial CO_2/H_2O ratio dropped to 0.5 or lower, the gas release changed substantially, with peaks being observed around 100 K and at 146 and 165 K. The amorphous ice obviously reconstructs in the temperature range 100−120 K, which enhances diffusion and subsequent release of CO_2. These earlier studies clearly illustrate the dynamic nature of amorphous ice at temperatures above 100 K, and the results are consistent with the efficient trapping and reversible release of CO_2 from amorphous ice observed in the present study.

Water and carbon dioxide are present in relatively large amounts at low temperatures in a variety of places, including the terrestrial atmosphere, the atmosphere and the poles of Mars, comets, and dense regions of interstellar space. An important question is whether mixed H_2O/CO_2 particles are formed or not under these different conditions. The Arrhenius parameters determined for CO_2 desorption in the present study can be used to estimate the surface coverage of CO_2 on ice under different conditions. The terrestrial atmosphere is very dry above the troposphere, but water ice particles may form if the temperature becomes sufficiently low. Temperatures down to 185 K in the stratosphere result in the formation of polar stratospheric clouds at an altitude of about 15−20 km, which play an important role in the formation of the "ozone hole" over Antarctica.[22] Using a CO_2 pressure of 4.5×10^{-2} mbar (altitude 15 km) and $T =$ 185 K, the surface coverage of CO_2 on stratospheric water ice particles is estimated to be 5×10^{-4}. This low surface coverage should not have a strong effect on heterogeneous chemistry in the stratosphere. This is in agreement with earlier estimates by Elliott et al.[23] It is, however, unlikely that pure water ice surfaces will exist under stratospheric conditions, and further studies should evaluate the effect of surface contaminants such as HCl on CO_2–ice interactions.

Noctilucent clouds are formed in the mesopause region at an altitude of about 85 km when the temperature drops to 100−

135 K,[24] and the cloud particles are believed to mainly consist of water. At these high altitudes the pressure of CO_2 is about 100−1000 times higher than the H_2O pressure, which raises the question of whether CO_2 may be incorporated in the ice particles or not. Using $T = 100$ K, a CO_2 pressure of 5×10^{-7} mbar (altitude 85 km), and the experimental data for crystalline ice, the surface coverage of CO_2 on ice particles in the mesopause region is estimated to be 7×10^{-4}. However, if we instead use the data for trapped molecules on amorphous ice, the surface coverage may be larger than 1 ML at 100 K. The ice structure of the ice particles can thus have a significant effect on CO_2 adsorption, and further studies of the properties of ice particles in the mesopause region are required.

Conclusions

Time-resolved molecular beam studies of carbon dioxide collisions with water ice shows that the gas−surface interactions are highly inelastic, and that trapping−desorption of CO_2 completely dominates in the temperature range 100−160 K. The desorption kinetics on crystalline ice at 100−125 K are well described by the Arrhenius equation with an activation energy of 0.22 ± 0.02 eV and a preexponential factor of $10^{13.32\pm0.57}$ s^{-1}. Amorphous ice formed at temperatures below 120 K is able to trap a substantial amount of CO_2 during minutes, while this does not take place on crystalline ice. The results imply that atmospheric crystalline ice particles are covered by CO_2 to an extent of less that 1‰. If, however, amorphous ice particles are formed, the coverage can extend up to monolayer thichness in the cold mesopause region. Further studies with other gases are currently under way to better characterize the processes taking place in amorphous ice at 100−120 K.

Acknowledgment. This work was supported by the Swedish Research Council.

References and Notes

(1) Andersson, P. U.; Någård, M. B.; Bolton, K.; Svanberg, M.; Pettersson, J. B. C. *J. Phys. Chem. A* **2000**, *104*, 2681.
(2) Gotthold, M. P.; Sitz, G. O. *J. Phys. Chem B* **1998**, *102*, 9557.
(3) Andersson, P. U.; Någård, M. B.; Pettersson, J. B. C. *J. Phys. Chem. B* **2000**, *104*, 1596.
(4) Rieley, H.; Aslin, H. D.; Haq, S. *J. Chem. Soc., Faraday Trans.* **1995**, *91*, 2349.
(5) Isaksson, M. J.; Sitz, G. O. *J. Phys. Chem. A* **1999**, *103*, 2044.
(6) Bolton, K.; Svanberg, M.; Pettersson, J. B. C. *J. Chem. Phys.* **1999**, *110*, 5380.
(7) Bolton, K.; Pettersson, J. B. C. *Chem. Phys. Lett.* **1999**, *312*, 71.
(8) Kroes, G.-J.; Clary, D. C. *J. Phys. Chem.* **1992**, *96*, 7079.
(9) Wang, L.; Clary, D. C. *J. Chem. Phys.* **1996**, *104*, 5663.
(10) Al-Halabi, A.; Kleyn, A. W.; Kroes, G. J. *Chem. Phys. Lett.* **1999**, *307*, 505.
(11) Bryson, C. E.; Levenson, L. L. *Surf. Sci.* **1974**, *43*, 29.
(12) Bar-Nun, A.; Herman, G.; Laufer, D.; Rappaport, M. L. *Icarus* **1985**, *63*, 317.
(13) Sandford, S. A.; Allamandola, L. J. *Astrophys. J.* **1990**, *355*, 357.
(14) Hudson, R. L.; Donn, B. *Icarus* **1991**, *94*, 326.
(15) Sack, N. J.; Baragiola, R. A. *Phys. Rev. B* **1993**, *48*, 9973.
(16) Westley, M. S.; Baratta, G. A.; Baragiola, R. A. *J. Chem. Phys.* **1998**, *108*, 3321.
(17) Haynes, D. R.; Tro, N. J.; George, S. M. *J. Phys. Chem.* **1992**, *96*, 8502.
(18) Stevenson, K. P.; Kimmel, G. A.; Dohnálek, Z.; Smith, R. S.; Kay, B. D. *Science* **1999**, *283*, 1505.
(19) Dohnálek, Z.; Kimmel, G. A.; Ciolli, R. L.; Stevenson, K. P.; Smith, R. S.; Kay, B. D. *J. Chem. Phys.* **2000**, *112*, 5932.
(20) Ayotte, P.; Smith, R. S.; Stevenson, K. P.; Dohnálek, Z.; Kimmel, G. A.; Kay, B. D. *J. Geophys. Res.* **2001**, *106*, 33387.
(21) Kimmel, G. A.; Stevenson, K. P.; Dohnálek, Z.; Smith, R. S.; Kay, B. D. *J. Chem. Phys.* **2001**, *114*, 5284.
(22) Farman, J. C.; Gardiner, B. G.; Shanklin, G. D. *Nature* **1985**, *315*, 207.
(23) Elliott, S.; Turco, R. P.; Toon, O. B.; Hamill, P. *J. Atmos. Chem.* **1991**, *13*, 211.
(24) Witt, G. *The nature of noctilucent clouds*; Space Research IX; North-Holland Publishing Co.: Amsterdam, 1969.